

Estimation of Rainfall Based on the Results of Polarimetric Echo Classification

SCOTT E. GIANGRANDE AND ALEXANDER V. RYZHKOV

Cooperative Institute for Mesoscale Meteorological Studies, University of Oklahoma, and NOAA/OAR National Severe Storms Laboratory, Norman, Oklahoma

(Manuscript received 4 April 2007, in final form 29 January 2008)

ABSTRACT

The quality of polarimetric radar rainfall estimation is investigated for a broad range of distances from the polarimetric prototype of the Weather Surveillance Radar-1988 Doppler (WSR-88D). The results of polarimetric echo classification have been integrated into the study to investigate the performance of radar rainfall estimation contingent on hydrometeor type. A new method for rainfall estimation that capitalizes on the results of polarimetric echo classification (EC method) is suggested. According to the EC method, polarimetric rainfall relations are utilized if the radar resolution volume is filled with rain (or rain and hail), and multiple $R(Z)$ relations are used for different types of frozen hydrometeors. The intercept parameters in the $R(Z)$ relations for each class are determined empirically from comparisons with gauges. It is shown that the EC method exhibits better performance than the conventional WSR-88D algorithm with a reduction by a factor of 1.5–2 in the rms error of 1-h rainfall estimates up to distances of 150 km from the radar.

1. Introduction

Accurate rainfall estimates are vital for most hydrologic applications. The U.S. National Weather Service (NWS) requires estimates of rainfall at ranges up to 230 km from the radar (WSR-88D Radar Operations Center 2001, section 3.7.2.2.1). However, the quality of radar measurements and rainfall estimates degrades with distance as a result of beam broadening and the effect of Earth curvature (e.g., Smith et al. 1996; Sanchez-Diezma et al. 2000; Ryzhkov 2007). At longer distances from the radar (typically beyond 100 km at base tilt), the radar resolution volume is more likely to be filled with mixed-phase or frozen hydrometeors. The radar measurements aloft are also very loosely related to rainfall near the ground as a result of drastic changes in microphysical properties of precipitation in the vertical due to sublimation, riming, aggregation, evaporation, coalescence, breakup, and advection (e.g., Doviak and Zrnich 1993, section 8.4).

Contamination from nonliquid hydrometeors is especially pronounced in colder climates where the melting layer (or bright band) is particularly low. Even in relatively warm climates, this contamination generally oc-

curs over a significant portion of the required NWS radar rainfall coverage area. For a typical warm-season melting level height in central Oklahoma (~3 km AGL), contamination of radar rainfall estimates at the 0.5° elevation angle due to the presence of mixed-phase and frozen hydrometeors is usually observed as close as 120 km from the radar. As a result, the accuracy of rain estimation may be compromised in over two-thirds of the radar rainfall coverage area required by the NWS.

Several studies discuss the quality of conventional rainfall estimation with single-polarization radar to large distances (e.g., Fabry et al. 1992; Smith et al. 1996; Seo et al. 2000; Krajewski and Ciach 2005). To obtain accurate surface rainfall measurements at longer distances, it is necessary to address the impact of melting-layer and frozen-hydrometeor contamination on radar measurements. For conventional radars, emphasis has been on establishing characteristic vertical profiles of reflectivity (VPR) to account for the reflectivity behavior through regions of melting hydrometeors (e.g., Koistinen 1991; Andrieu and Creutin 1995; Kitchen 1997). Although methods capitalizing on the knowledge of the VPR yield improved rainfall estimates at longer distances, these techniques are sensitive to precipitation variability, including changes in storm type (e.g., stratiform vs convective) and temporal/spatial changes in the VPR (e.g., Zawadzki 2006). In this study, we suggest an alternate approach that capitalizes on

Corresponding author address: Scott Giangrande, CIMMS/NSSL, 120 David L. Boren Blvd., Norman, OK 73072.
E-mail: scott.giangrande@noaa.gov

polarimetric classification of radar echo rather than vertical profiles of reflectivity.

Polarimetric radar provides new opportunities to improve the accuracy of rain measurements as numerous theoretical and validation studies show (e.g., Ryzhkov and Zrnić 1996; May et al. 1999; Bringi and Chandrasekar 2001; Brandes et al. 2002; Matrosov et al. 2005; Ryzhkov et al. 2005b). Polarimetric rainfall estimation techniques are more robust with respect to drop size distribution (DSD) variations and the presence of hail than are the conventional $R(Z)$ relations (here, R is radar rainfall rate and Z is reflectivity). The measurements of specific differential phase K_{DP} , which is immune to radar miscalibration, attenuation, and partial beam blockage (Zrnić and Ryzhkov 1996), benefit the quality of precipitation estimation by providing methods to correct radar reflectivity biases that result from those listed factors or through the direct estimation of rainfall using $R(K_{DP})$ relations. In addition, polarimetric radar is uniquely suited for discriminating among different classes of meteorological and nonmeteorological echo (e.g., Zrnić and Ryzhkov 1999; Vivekanandan et al. 1999; Liu and Chandrasekar 2000; Zrnić et al. 2001; Lim et al. 2005), which may also benefit estimates of rain. The anticipated improvement in quantitative precipitation estimation is one of the primary motivations for the forthcoming polarimetric upgrade of the Weather Surveillance Radar-1988 Doppler (WSR-88D) network (e.g., Ryzhkov et al. 2005c).

A number of different polarimetric algorithms for rainfall estimation have been recently validated in an operational environment during the Joint Polarization Experiment (JPOLE) field campaign, which was held in central Oklahoma in 2002–03 (Ryzhkov et al. 2005b,c). In the JPOLE study, it was shown that the so-called synthetic algorithm, which utilizes different polarimetric relations depending on the value of Z , outperforms all other relations at the distances less than 90 km from the radar (Ryzhkov et al. 2005b). The performance of the synthetic algorithm (as well as other rainfall algorithms) at longer ranges was not investigated in that study. Preliminary analysis by Giangrande and Ryzhkov (2003) and Ryzhkov et al. (2005c) demonstrated statistical improvement in the accuracy of rain measurements at longer distances (between 100 and 200 km) if the $R(K_{DP})$ relation is used instead of $R(Z)$. We are not aware of any other substantial effort to validate polarimetric rainfall algorithms beyond the range of 100 km, and the quality of polarimetric rainfall measurements at longer distances (where the radar samples mixed-phase and frozen hydrometeors) is largely unknown. One of the major objectives of this paper is to examine the performance of polarimetric

algorithms for rain estimation up to the distance of 250 km from the radar using a large dataset collected with the polarimetric prototype of the WSR-88D radar (referred to by identifier KOUN herein) and Oklahoma Mesonet gauge network.

Previous studies indicate that regardless of range interval it is unlikely any single radar relation would produce high-quality precipitation estimates at different distances from the radar and for different types of hydrometeors filling the radar resolution volume (e.g., Jameson 1991; Chandrasekar et al. 1993; Cifelli et al. 2002; Ryzhkov et al. 2005b). According to the Ryzhkov et al.'s (2005b) synthetic approach, the segregation between different polarimetric relations is based on radar reflectivity factor. Following Zrnić (1996), we suggest using results of polarimetric hydrometeor classification for such a segregation.

This paper assesses the quality of polarimetric rainfall estimation for a broad range of distances from the radar. The data were collected with the KOUN radar in central Oklahoma. Polarimetric echo classification has been integrated into this study to investigate the performance of radar rainfall estimation contingent on the type of hydrometeors that fill the radar resolution volume. Hourly Agricultural Research Service (ARS) Miconet and Oklahoma Mesonet rain gauge accumulations are used to validate conventional and polarimetric radar rainfall measurements (e.g., Brock et al. 1995; Shafer et al. 2000). The ARS and Oklahoma Mesonet gauges used in this study are well calibrated and are located at distances between 25 and 250 km from the KOUN radar (e.g., Shafer et al. 2000; Fiebrich et al. 2006; McPherson et al. 2007).

2. Radar dataset, preprocessing, and echo classification

A total of 43 events observed by the KOUN radar between 2002 and 2005 have been selected for analysis. The dataset includes gauge observations from over 100 Oklahoma Mesonet stations and comprises 179 h of radar data. Concurrent gauge observations were available from the densely spaced ARS network stations located at ranges of 50–88 km from the KOUN radar. The total number of ARS gauges is 42 (24 after 2004 when some gauges were decommissioned), with an average spacing of about 5 km. Over the ARS network, comparisons between the performance of radar-based rainfall retrievals are mainly affected by DSD variability and the possible presence of hail rather than ground clutter or contamination from the melting layer or frozen hydrometeors (e.g., Ryzhkov et al. 2005b). A map of the observation network in central Oklahoma is presented in Fig. 1. A complete list of rain events and

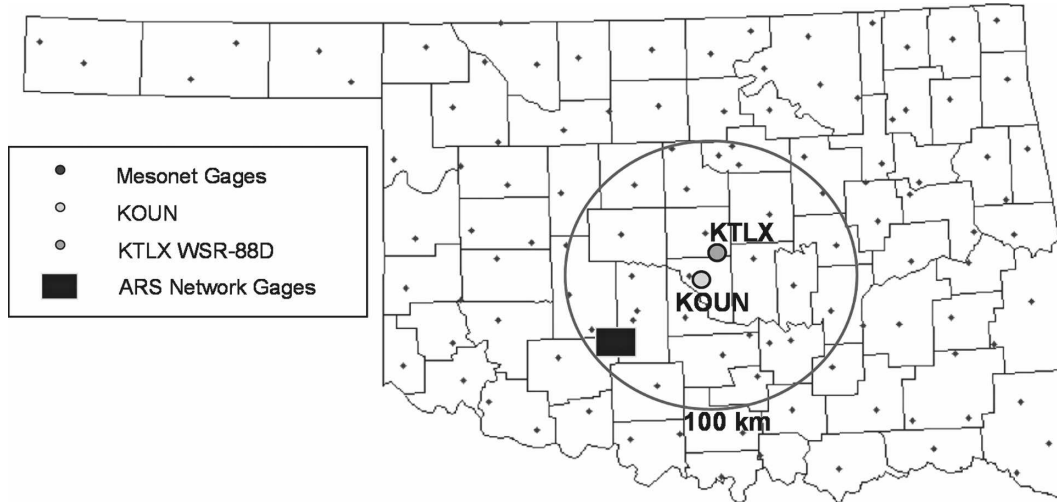


FIG. 1. Map of the observation network in central Oklahoma.

hours of observation is provided in Table 1. The dataset includes warm-season convective storms containing hail, mesoscale convective systems (MCS) with intense squall lines and trailing stratiform precipitation, widespread cold-season stratiform rain, and select tropical storm remnants. The Mesonet and ARS gauges (shielded Met One Instruments, Inc., tipping-bucket type) used in the study are unheated; therefore we exclude the data associated with frozen and/or mixed-phase precipitation recorded at gauge level.

Radar reflectivity factor at horizontal polarization Z , differential reflectivity Z_{DR} , specific differential phase K_{DP} , and cross-correlation coefficient ρ_{HV} were measured at a radial resolution of 0.250–0.267 km using a short dwell time (48 radar samples) to satisfy Next-Generation Weather Radar (NEXRAD) antenna rotation rate (3 revolutions per minute) and azimuthal resolution (1°) requirements. Radar rainfall estimates and echo classification results were obtained using data collected at the 0.5° elevation scan with an update time varying between 2 and 6 min. Radar reflectivity measured by KOUN was matched with Z obtained from the nearby KTLX WSR-88D radar, which was assumed to be well calibrated based on the results of our previous studies (e.g., Ryzhkov et al. 2005a; Giangrande and Ryzhkov 2005). Differential reflectivity Z_{DR} was calibrated using polarimetric signatures of dry aggregated snow above the melting level following Ryzhkov et al. (2005a). Attenuation correction of Z and Z_{DR} was performed using differential phase Φ_{DP} and relations ΔZ (dB) = $0.04\Phi_{DP}$ ($^\circ$) and ΔZ_{DR} (dB) = $0.004\Phi_{DP}$ ($^\circ$) (Ryzhkov and Zrnić 1995). Two estimates of K_{DP} are obtained from a filtered Φ_{DP} as a slope of least squares fit for two range averaging intervals, corresponding to 9

and 25 successive gates. For any particular gate, the lightly filtered K_{DP} estimate is selected if $Z > 40$ dBZ, and otherwise the heavily filtered K_{DP} is selected (Ryzhkov and Zrnić 1996). A minimum $\rho_{HV} = 0.85$ threshold was applied to filter echoes of nonmeteorological origin. Radar reflectivity was capped at 53 dBZ to mitigate hail contamination. Additional details of data processing can be found in Ryzhkov et al. (2005c).

In this study we compare hourly gauge and radar rainfall accumulations over gauge locations within 250 km of KOUN. Hourly radar accumulations are defined as an hourly rainfall estimate averaged over an area centered on an individual gauge. Radar rain rates are averaged using five gates centered over the gauge location and two closest azimuths separated by 1° . Such averaging produces a radial resolution of 1.0 km and transverse resolution that varies with range.

To establish the quality of the conventional and polarimetric radar rainfall algorithms, absolute differences between radar and gauge estimates (expressed in millimeters) are examined rather than standard fractional errors, which are heavily weighted toward small accumulations. Rainfall estimates are characterized by the bias $B = \langle \Delta \rangle$ and the rms error $RMSE = \langle |\Delta|^2 \rangle^{1/2}$, where $\Delta = T_R - T_G$ is the difference between radar and gauge hourly totals for any given radar–gauge pair and angle brackets imply averaging over all such pairs.

When comparing radar and gauge rain estimates, one must be mindful of the errors of tipping-bucket gauge measurements (e.g., Zawadzki 1975; Wilson and Brandes 1979; Austin 1987; Ciach 2003). The errors in gauge accumulations associated with high-wind undercatch and splashing may exceed 12% for intense MCS events in central Oklahoma (Duchon and Essenberg

TABLE 1. Listing of KOUN events and the hours of observation.

No.	Date	Hours (UTC)	Event type
1	14 Aug 2002	1–4	MCS
2	8 Sep 2002	18–21	Tropical remnant
3	9 Sep 2002	16–17	Tropical remnant
4	14 Sep 2002	6–11	MCS
5	19 Sep 2002	2–7	MCS
6	8 Oct 2002	17–20, 22–23	Widespread stratiform
	9 Oct 2002	1–3, 4–5, 13–14	
7	19 Oct 2002	19–20, 21–22	Widespread stratiform
8	24 Oct 2002	15–17, 19–21	Widespread stratiform
9	28 Oct 2002	19–20	Widespread stratiform
10	3 Dec 2002	22–23	Stratiform/ice northwest of Oklahoma City
	4 Dec 2002	1–3	
11	19 Apr 2003	10–14	MCS
12	23 Apr 2003	22–23	Isolated convection
13	14 May 2003	5–11	Severe convective cells
14	16 May 2003	5–10	MCS
15	20 May 2003	1–5	Isolated convection
16	2 Jun 2003	3–6	MCS
17	4 Jun 2003	12–14, 15–17	MCS
18	5 Jun 2003	10–15	MCS
19	6 Jun 2003	2–7	MCS
20	11 Jun 2003	0–1, 2–6	MCS
21	12 Jun 2003	0–5	MCS
22	13 Jun 2003	10–14	Isolated convection
23	24 Apr 2004	2–7	MCS
24	13 May 2004	19–20	MCS
25	2 Jun 2004	20–23	MCS
26	4 Jun 2004	14–20	Isolated convection
27	19 Jun 2004	16–20	MCS
28	21 Jun 2004	8–13	MCS
29	22 Jun 2004	8–12	MCS
30	28 Aug 2004	8–12	MCS
31	14 Nov 2004	20–23	Widespread stratiform
32	15 Nov 2004	10–14	Widespread stratiform
33	13 May 2005	6–10	MCS
34	27 May 2005	15–18	Isolated convection
35	5 Jun 2005	1–5	MCS
36	10 Jun 2005	7–11	MCS
37	17 Jun 2005	4–7	MCS
38	1 Jul 2005	14–17	MCS
39	27 Aug 2005	18–22	Isolated convection
40	29 Aug 2005	3–6	Isolated convection
41	14 Sep 2005	3–6	MCS
42	1 Oct 2005	2–18	MCS
43	5 Oct 2005	21–23	MCS
	6 Oct 2005	0–3, 4–6	

2001). These errors are not common and/or typically have a lesser impact on the hourly rain total. Quality-assurance meteorologists at the Oklahoma Mesonet perform regular gauge maintenance and event-based analysis to detect and remove accumulation reports from malfunctioning and apparently biased gauges. Thus, we believe that the intrinsic gauge errors in the hourly rain total are well below the expected errors of radar rainfall measurements.

An objective of this study is to examine the quality of radar rain measurements as a function of radar echo type and to explore the value of polarimetric hydrometeor classification for quantitative precipitation estimation. For this purpose, the type of scatterers in the radar sampling volume corresponding to a particular gauge location was identified using a polarimetric classification algorithm based on fuzzy-logic principles. The classification algorithm utilized herein is close to the one described by Ryzhkov et al. (2007) and Park et al. (2007). The membership functions in the fuzzy-logic scheme are consistent with those in the literature (e.g., Liu and Chandrasekar 2000; Lim et al. 2005). The classifier distinguishes among 10 classes of radar echo, including anomalous propagation and ground clutter (AP/GC), biological scatterers (BS), light to moderate rain (RA), heavy rain (HR), rain–hail (RH), big drops (BD), graupel (GR), wet snow (WS), dry snow (DS), and ice crystals (CR). The classification algorithm in this study utilizes four radar variables: Z , Z_{DR} , ρ_{HV} , and a texture parameter $SD(Z)$, that is, the standard deviation of small-scale fluctuations of Z along a radial; $SD(Z)$ is primarily used to distinguish between meteorological and nonmeteorological echo.

In addition to radar variables, the fuzzy-logic algorithm also utilizes information about the vertical temperature profile or melting-layer depth for better delineation of the areas of liquid, mixed-phase, and frozen hydrometeors. The parameters of the melting layer can be determined from soundings, numerical model output, or polarimetric radar data themselves (e.g., Giangrande et al. 2008). When performing echo classification at grazing angles, it is necessary to consider the impact of beam broadening for proper echo designation relative to melting-layer boundaries. Here, we define the minimal slant range for which the entire radar resolution volume is above the freezing level as R_r . In a similar way, the maximal slant range at which the entire radar resolution volume is located below the bottom of the melting layer is defined as R_b . Different class designations are allowed depending on the slant range at a given elevation (Ryzhkov et al. 2007). For example, wet snow is only allowed between R_b and R_r .

The classification code distinguishes among four types of rain: RA, HR, RH, and BD. The membership functions in the fuzzy-logic scheme for four classes of rain overlap significantly in terms of all four radar variables and are constructed in such a way that distinction between RA and HR is primarily based on Z using a 45-dBZ borderline. This corresponds to a rain rate of approximately 25–30 mm h⁻¹. Rain–hail mixture RH, on the other hand, is recognized and distinguished from HR with the same Z by significantly lower values of

TABLE 2. The results of echo classification for the Oklahoma Mesonet dataset. Percentages exclude nonecho/null classifications. The $\langle R \rangle$ and $\langle Z_{DR} \rangle$ are mean values of rainfall rate (Z capped at 53 dBZ) and differential reflectivity over gauge locations for the corresponding echo class. The standard NEXRAD $R(Z)$ relation (1) is used to estimate the relative contribution to the total radar-estimated rain depth in the far-right column.

Echo category	No. obs	Occurrence (%)	$\langle R \rangle$ capped (mm h^{-1})	$\langle Z_{DR} \rangle$ (dB)	Contribution to $R(Z)$ rainfall (%)
GC/AP	7736	9.79	2.88	0.62	5.94
Biological	11 577	14.66	0.34	2.89	0.89
Dry snow	4560	5.78	1.51	0.48	1.59
Crystals	1251	1.58	0.50	0.81	0.14
Wet snow	9443	11.96	5.03	1.10	10.75
Graupel	2695	3.41	14.41	0.60	8.93
Rain	34 016	43.08	3.68	0.83	28.9
Big drops	4989	6.31	3.93	1.66	4.48
Heavy rain	2224	2.82	58.58	2.11	29.7
Rain-hail	460	0.58	82.33	1.15	8.65

Z_{DR} and ρ_{HV} . Rain associated with significant presence of big drops and/or a relative deficit of small drops is usually characterized by anomalously high Z_{DR} (for a given Z) and is identified as BD in the echo classifier. Rain belonging to the BD category is commonly observed in the updraft areas of the storms where vigorous size sorting of raindrops occurs; BD designations may also be found beneath mature bright bands associated with the melting of large snowflakes in the stratiform regions of an MCS.

Table 2 and Fig. 2 summarize results of echo classification at Oklahoma Mesonet gauge locations up to 250 km from the KOUN radar for the entire dataset containing 43 rain events and 179 h of observation. On average, a radar echo over a particular gauge was strong enough to be classified during 30% of the observation period.

The second column in Table 2 shows the percentage of occurrence for different echo types at elevation 0.5° in the 250-km radius area for the whole dataset. These data indicate that about 53% of radar echoes observed at the lowest elevation scan are associated with liquid hydrometeors and/or rain mixed with hail and that wet snow or frozen particles are responsible for 23% of these echoes. Classification performed over the ARS gauges at the lowest elevation angle shows an absence of frozen and mixed-phase echo for the events in the dataset.

For the classifications over Oklahoma Mesonet gauge locations, the RA category is the dominant echo type and is classified to the distances of 170 km. Although convective rain categories including heavy rain, big drops, and rain-hail only account for approximately 10% of the valid classifications, their contribution to total rain amount exceeds 40% [if estimated from the standard WSR-88D $R(Z)$ relation] because of higher rain rates. Echoes related to frozen and mixed-phase hydrometeors are typically observed at distances be-

yond 100 km. Wet snow is a prevalent category among nonrain class designations owing to several MCSs with trailing stratiform precipitation in the dataset.

Echo classification is performed over each gauge location during every radar scan, whereas radar and gauge rainfall accumulations are computed for each hour. Because classification results generally change from scan to scan at the same location, several class designations may be associated with a single hourly rain total. To quantify the accuracy of hourly rainfall estimation for individual echo classes, we prefer to assign the hourly rain total to a single, dominant echo class for that hour. For example, a particular hourly gauge accumulation is associated with RA if the corresponding radar echo is classified as RA for at least 70% of radar scans constituting this hour. We refer to this type of echo as rain type I. The gauge hours that do not meet this requirement are removed from the statistics.

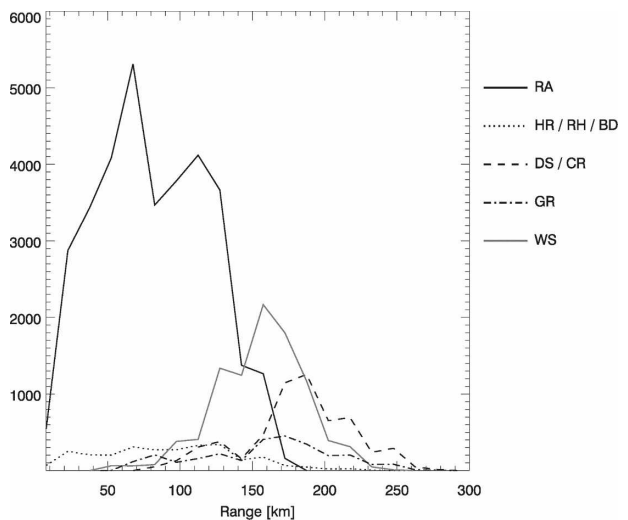


FIG. 2. Histogram of ranges associated with different classes of hydrometeors observed at the 0.5° elevation.

Other categories of rain (BD, HR, RH) are relatively infrequent (see Fig. 2 and Table 2), and the number of hours and gauges over which such signatures are dominant is too small for obtaining reliable statistics. For this reason, we combine these rain categories in a single class of rain called rain type II. An hourly gauge total is associated with rain type II if any of RA, BD, HR, or RH (or some or all of them together) are detected for at least 70% of the time and one of the three categories BD, HR, or RH is identified for no less than 20% of the time.

3. Rainfall estimates associated with different echo types

The performance of different rainfall relations is investigated, contingent on the results of polarimetric echo classification. It is known that conventional radar rainfall estimates obtained from $R(Z)$ relations deteriorate in the presence of mixed-phase and frozen hydrometeors. Previous studies have shown that the $R(Z, Z_{DR})$ relation is less prone to DSD variability, but it is not immune to hail contamination and is not efficient in situations of melting-layer contamination and precipitation overshooting (e.g., Aydin et al. 1990; Ryzhkov and Zrnić 1995; Brandes et al. 2002; Ryzhkov et al. 2005b,c). Rainfall algorithms based on K_{DP} are more robust in the presence of hail but are not optimal for light rain at S band (e.g., Chandrasekar et al. 1990; Ryzhkov and Zrnić 1995). Giangrande and Ryzhkov (2003) demonstrate that $R(K_{DP})$ outperforms $R(Z)$ in melting-layer regions, but the improvement may be fortuitous and requires further clarification. The results of polarimetric echo classification can be utilized to further investigate the nature of the errors inherent to all three types of rainfall relations [$R(Z)$, $R(Z, Z_{DR})$, and $R(K_{DP})$] depending on the type of radar echo. We examine the performance of different rainfall relations separately in rain below the melting layer, within the melting layer where wet snowflakes are the dominant scatterers, and in frozen hydrometeors including graupel, hail, dry snow, and crystals above the melting layer where the direct application of radar rainfall relations is questionable.

a. Rainfall relation comparisons in rain

Rain is most often classified at relatively close distances from the radar. For this reason, both Oklahoma Mesonet and ARS Micronet gauge network accumulations are available to validate radar rainfall algorithms in rain. In this study, the following $R(Z)$, $R(K_{DP})$, and $R(Z, Z_{DR})$ relations have been selected for analysis:

$$R(Z) = (1.7 \times 10^{-2})Z^{0.714}, \quad (1)$$

$$R(K_{DP}) = 44.0|K_{DP}|^{0.822} \text{sign}(K_{DP}), \quad \text{and} \quad (2)$$

$$R(Z, Z_{DR}) = (1.42 \times 10^{-2})Z^{0.770}Z_{dr}^{-1.67}. \quad (3)$$

The conventional $R(Z)$ relation in (1) is the inversion of the standard NEXRAD formula $Z = 300R^{1.4}$, where Z is expressed in millimeters to the sixth power per meter cubed and R is in millimeters per hour. In (2), K_{DP} is expressed in degrees per kilometer and the $\text{sign}(K_{DP})$ term allows negative values of R (e.g., Ryzhkov and Zrnić 1996). Lowercase subscript in Z_{dr} in (3) indicates linear units as opposed to uppercase subscript, which denotes logarithmic scale. Polarimetric relations (2) and (3) are selected because of their optimum performance in rain for central Oklahoma during the JPOLE field campaign (e.g., Ryzhkov et al. 2005b).

Scatterplots of hourly rainfall totals obtained from the radar relations (1)–(3) versus hourly gauge accumulations are displayed in Figs. 3–6. Figures 3 and 4 illustrate radar–gauge comparisons using Oklahoma Mesonet and ARS gauges if rain is classified as rain type I as specified in section 2. Similar plots highlighting the performance of the three rainfall relations for more convective and/or heavier rain type II (as specified in the previous section) are provided in Figs. 5 and 6 for the same gauge networks.

For rain type I, the tested relations show similar performance with respect to both gauge networks. A modest improvement in the rms errors is observed for all three rainfall relations if the ARS network is utilized for validation. This may be attributed to the improved spatial resolution of the KOUN radar measurements over these gauges (all 42 ARS gauges are located to within 88 km, as compared with 20 Oklahoma Mesonet gauges). As Figs. 3 and 4 show, the $R(Z, Z_{DR})$ relation is relatively unbiased and has the lowest rms errors over both networks, consistent with the Brandes et al. (2002) findings. The improvement yielded by the $R(Z, Z_{DR})$ is relatively modest for rain type I and is more pronounced over the ARS network (Fig. 4c).

There is a clear benefit in polarimetric rainfall estimation in rain type II. The sizable reduction in bias and rms error (as compared with rain type I) for the $R(Z, Z_{DR})$ and $R(K_{DP})$ relations is an indication that these relations are less susceptible to hail contamination and DSD variability. The conventional $R(Z)$ relation significantly overestimates rain type II even though radar reflectivity is capped at the 53-dBZ level to mitigate hail contamination. This overestimation is attributed to large raindrops and/or melting hailstones, which are typical for convective storms during the warm season in Oklahoma (e.g., Ryzhkov et al. 2005b). High values of

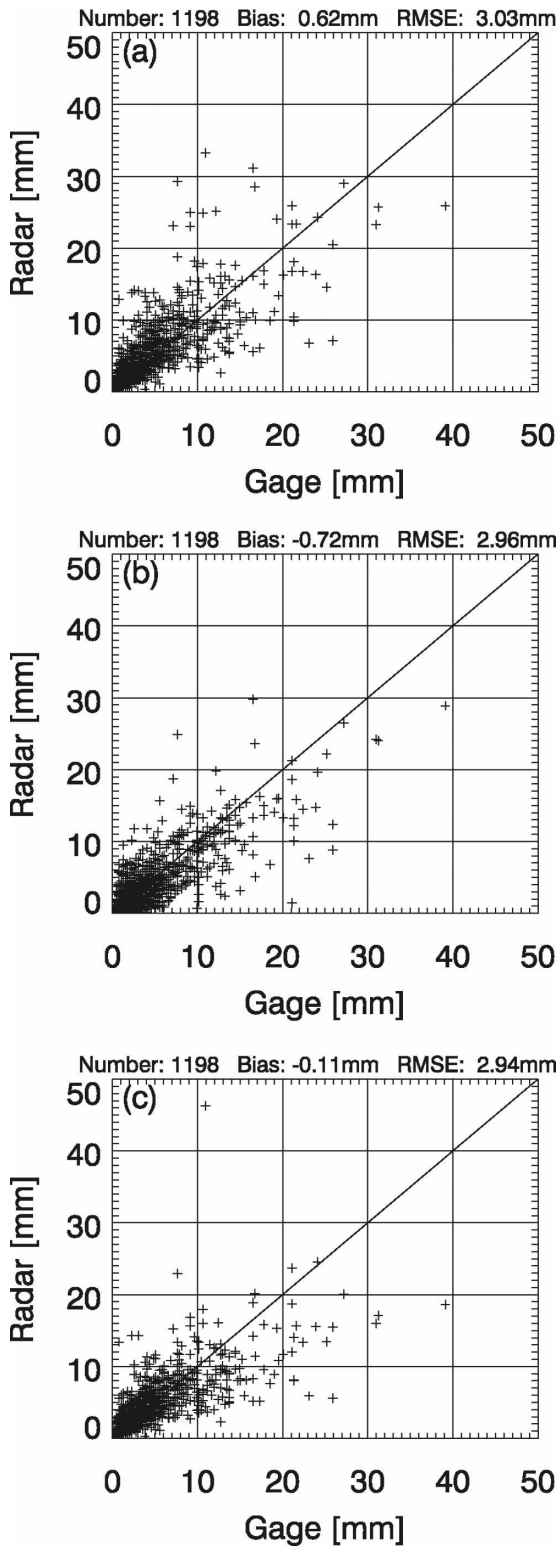


FIG. 3. Hourly radar–gauge rainfall accumulation scatterplots for rain type I over Oklahoma Mesonet gauge locations: (a) $R(Z)$, (b) $R(K_{DP})$, and (c) $R(Z, Z_{DR})$.

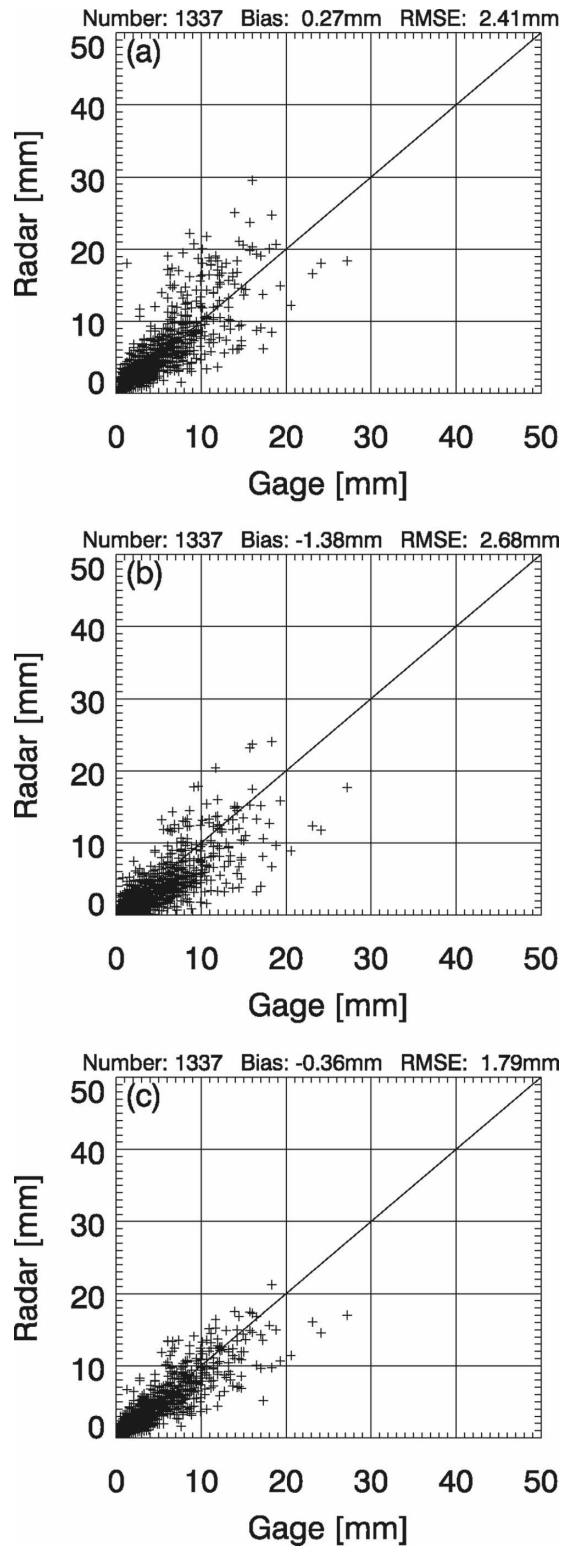


FIG. 4. As in Fig 3, but over ARS network gauge locations.

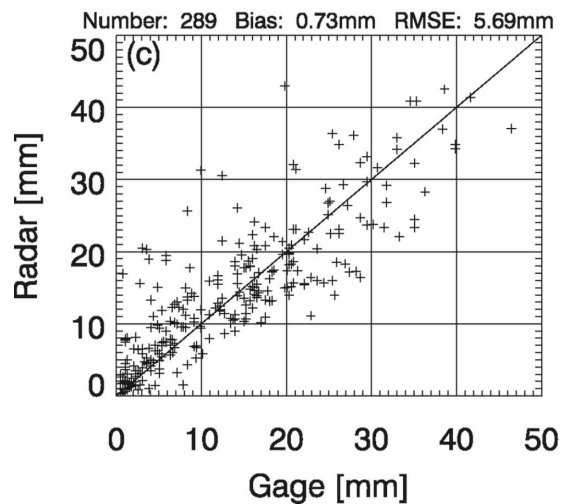
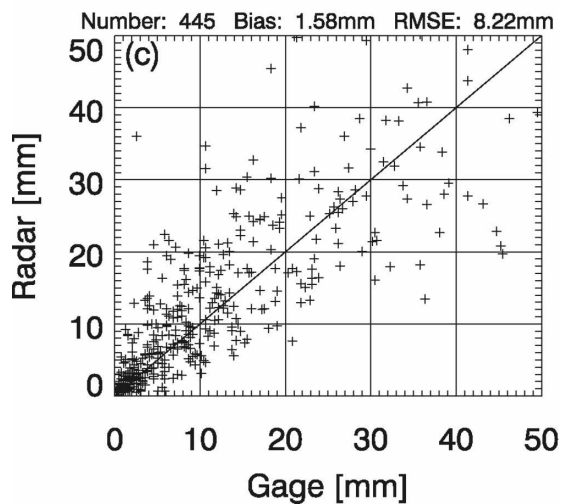
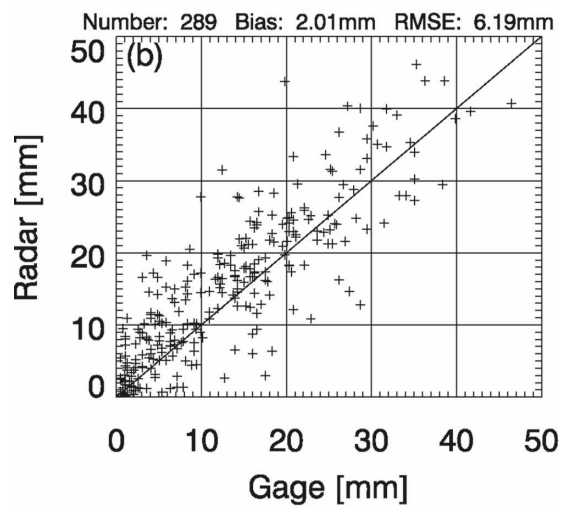
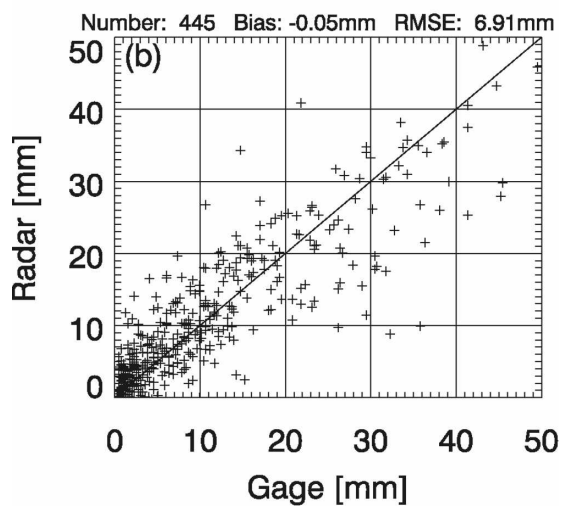
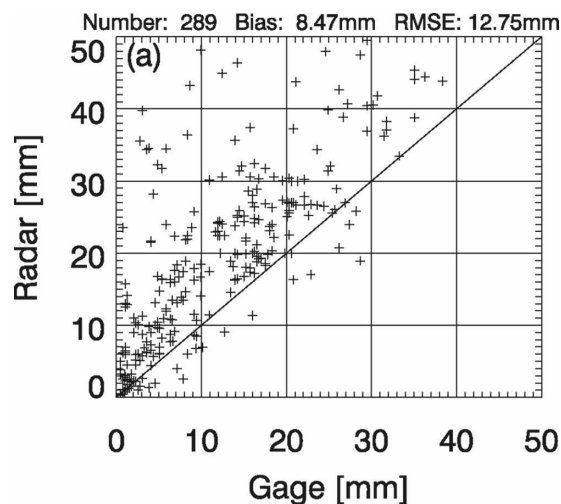
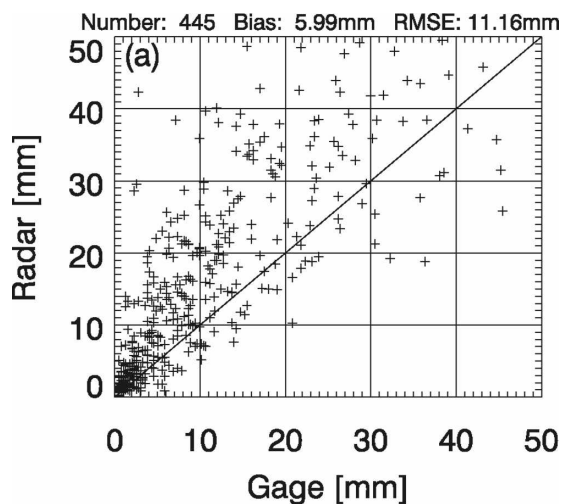


FIG. 5. As in Fig. 3, but for rain type II.

FIG. 6. As in Fig. 4, but for rain type II.

Z in the $R(Z, Z_{DR})$ relation from (3) are offset by large intrinsic Z_{DR} for big drops and/or small melting hail.

The performance of the $R(K_{DP})$ and $R(Z, Z_{DR})$ relations for rain type II is comparable, and network-relative performance is similar to the case of rain type I (Figs. 3, 4). At closer distances from the radar where the radar estimates are validated against ARS rain gauges (Figs. 6b,c), the $R(K_{DP})$ relation yields slightly higher bias and rms error relative to $R(Z, Z_{DR})$. The opposite is true in the broader range of distances where validation is performed using Oklahoma Mesonet gauges (Figs. 5b,c). The K_{DP} measurements are already heavily filtered in range, which may explain why these measurements are less sensitive to the additional beam broadening/filling effects in rain over mesonet gauges.

The choice between $R(K_{DP})$ and $R(Z, Z_{DR})$ in rain type II is affected by the quality of absolute calibration of Z and Z_{DR} , severity of the nonuniform beam filling (NBF) effects, and required spatial resolution of rain estimates. For example, the $R(Z, Z_{DR})$ relation cannot be applied in rain–hail mixtures if the increase in Z is not compensated by the proportional increase of Z_{DR} in (3). One has to distinguish between situations in which rain is mixed with relatively small melting hail having high Z_{DR} and large hail characterized by low Z_{DR} . According to our classification algorithm, only the latter situation is qualified as hail–rain mixture. This is confirmed by the difference in the $2^\circ \times 1$ km average values of $R(Z)$ and Z_{DR} for heavy rain and rain–hail in Table 2. In the rain–hail mixture, higher Z is associated with lower Z_{DR} and the $R(K_{DP})$ relation produces smaller bias.

Specific differential phase is immune to radar miscalibration and attenuation in rain, making $R(K_{DP})$ algorithms an attractive choice for rainfall estimation. However, because estimates of K_{DP} are noisier and more prone to NBF, the fields of $R(K_{DP})$ and even corresponding hourly totals may contain spurious perturbations and “holes” associated with unphysical negative rain rates or accumulations. An example of these holes in a rainfall accumulation display is presented in Fig. 7a. The reflectivity-based relation generally produces less noisy, “hole free” fields of rain totals and may be favorable for operational forecast/warning applications, which require high spatial and temporal resolution (Fig. 7b). The $R(K_{DP})$ relation may be preferred in hydrological applications, which need unbiased estimates of rain integrated over a large spatial/temporal domain.

b. Rainfall relation comparisons in wet snow

Wet Snow echoes are associated with (but not limited to) locations of pronounced brightband signatures in Z .

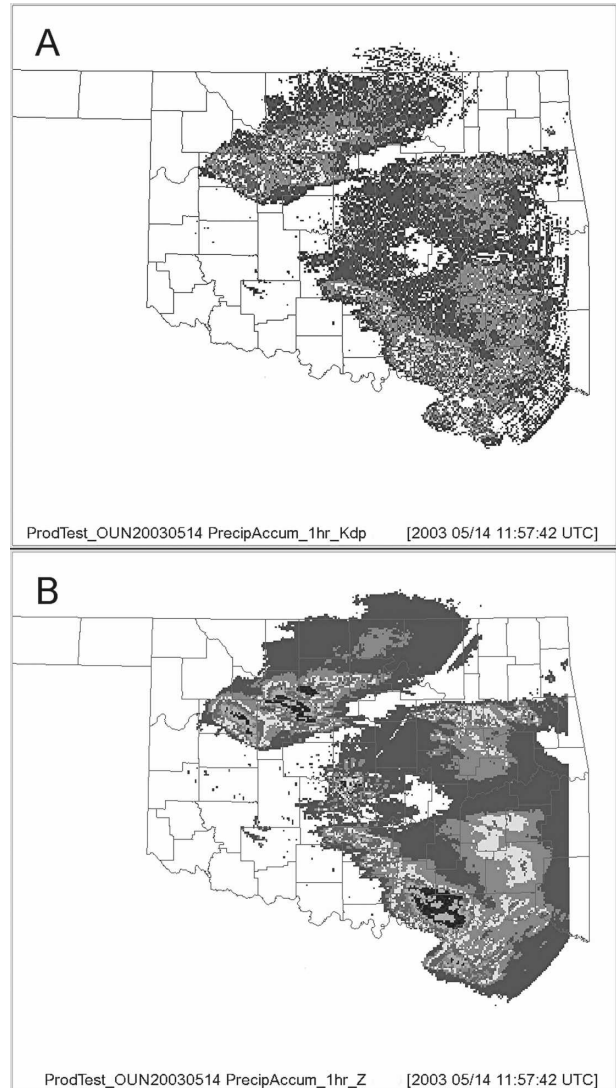


FIG. 7. An example of hourly rain accumulation maps obtained using an (a) $R(K_{DP})$ relation and (b) $R(Z)$ relation.

Wet snow is identified with greater confidence if Z is supplemented with polarimetric variables Z_{DR} and ρ_{HV} . For the KOUN radar, wet snow echoes are best characterized by values of ρ_{HV} between 0.90 and 0.97 and Z_{DR} values exceeding 0.7 dB.

The comparison between hourly rain totals obtained from (1)–(3) and Oklahoma Mesonet gauges in the cases in which the radar samples wet snow above the gauges is illustrated in Fig. 8. Again, an hourly rain total is associated with wet snow if the radar echo is classified as wet snow for at least 70% of the scans within the hour. Note that dry snow or RA radar echo, the echo classes that typically straddle the melting layer with height, may make up the remaining minority of the scans. At elevation 0.5° , wet snow in the radar resolu-

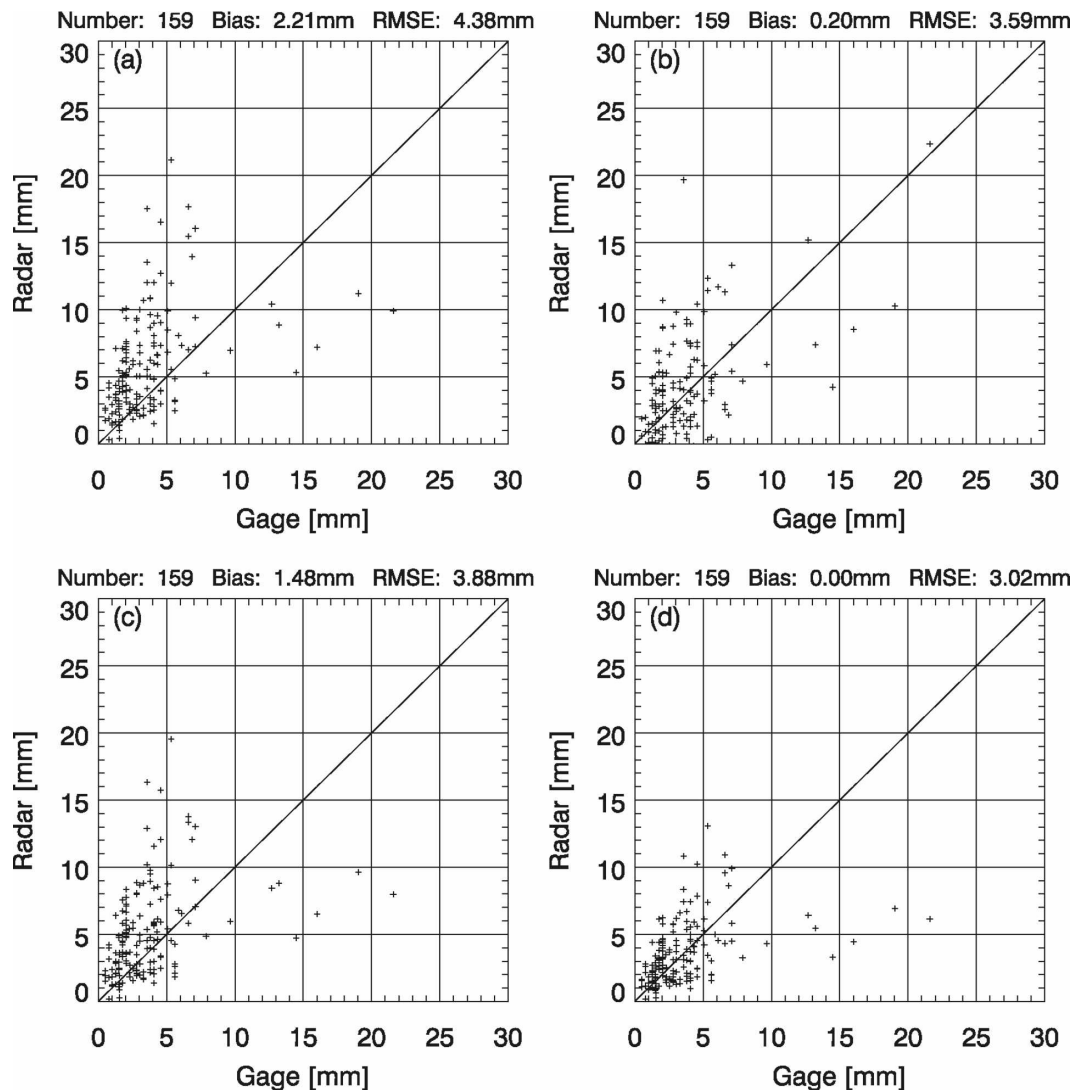


FIG. 8. Hourly radar–gauge rainfall accumulation scatterplots for wet snow over Oklahoma Mesonet gauges: (a) $R(Z)$, (b) $R(K_{DP})$, (c) $R(Z, Z_{DR})$, and (d) $0.6R(Z)$ that minimizes bias.

tion volume is usually classified at distances beyond 80 km from the radar and beyond the ARS Micronet gauge network (Fig. 1). Thus, ARS network accumulations cannot be used for validation in the case of wet snow echoes.

The use of a single $R(Z)$ rainfall relation through rain, mixed-phase, and snow regions is a common practice in conventional NEXRAD operations. However, no reasonable expectation exists that a single relation developed for the rain medium would be applicable to longer distances and through mixed-phase regions. As Fig. 8a shows, the conventional $R(Z)$ relation applied over wet snow echo gauges significantly overestimates surface rainfall. Slight improvement in terms of the bias and rms error is observed if polarimetric relations are used (Figs. 8b,c). Such an improvement may be ex-

plained by the fact that K_{DP} is less affected by the contribution from large wet snowflakes than is Z . Also, because Z_{DR} is high in wet snow, the combined use of Z and Z_{DR} helps to partially mitigate the overestimation inherent to $R(Z)$. However, the peaks in the vertical profiles of Z and Z_{DR} through the bright band generally do not coincide in height and Z and Z_{DR} do not correlate to the extent typical for ordinary rain. In addition, both K_{DP} and Z_{DR} are very prone to the NBF effects in the presence of very strong vertical gradients in the melting layer (Ryzhkov 2007) and are noisy because of low ρ_{HV} . Thus, the use of (2)–(3) in wet snow is not as beneficial as in rain, and additional study is required to determine the usefulness of these relations.

In view of these considerations, we recommend using a modified $R(Z)$ relation, as opposed to polarimetric

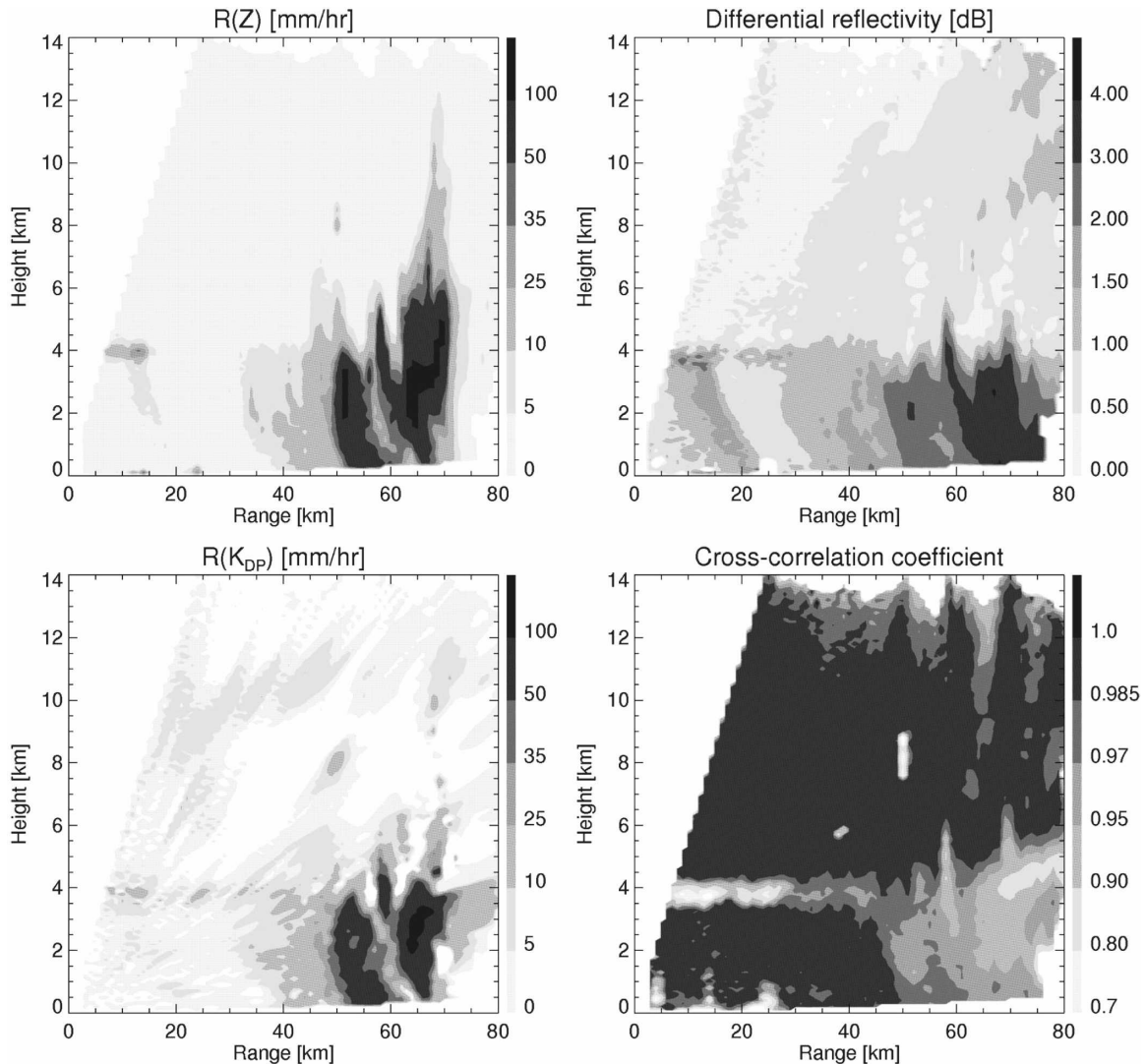


FIG. 9. Vertical cross section of $R(Z)$, Z_{DR} , $R(K_{DP})$, and ρ_{HV} through a thunderstorm, illustrating the loose connection between $R(K_{DP})$ and Z_{DR} aloft and rain at the surface.

relations, if the radar echo is classified as wet snow. Such a modification implies multiplying the right side of (1) by a factor that can be determined empirically by minimizing the bias and rms error in the rain estimate. In the case of wet snow for this dataset, this factor was determined to be 0.6; that is, the relation $R = 0.6R(Z)$ works the best (Fig. 8d).

c. Conventional-relation performance above the melting layer

The echo classification routine used in this study classifies four hydrometeor species above the melting layer: dry snow, crystals, graupel, big drops, and rain–hail. Dry snow and crystals encompass most polarimetric echo designations exhibiting low Z (generally less than

35 dBZ) and ρ_{HV} greater than 0.97. Discrimination between dry snow and crystals is primarily based on the magnitudes of Z and Z_{DR} . Discrimination between graupel and rain–hail above the melting layer is primarily based on the magnitudes of Z and ρ_{HV} . Big drops encompass most of the remaining liquid precipitation in updraft regions with ρ_{HV} greater than 0.97.

As illustrated by a polarimetric radar cross section through a typical Oklahoma thunderstorm (Fig. 9), the two polarimetric variables K_{DP} and Z_{DR} measured above the melting layer are noisy, are often negative, and seem loosely connected with rain on the ground. Although microphysical processes in the frozen part of the cloud directly impact rain formation and polarimetric measurements undoubtedly provide insight into the nature of such processes and snow type, the quantita-

tive use of the polarimetric variables measured above the melting layer for precipitation estimation on the ground has not yet been justified. At the moment, the use of modified $R(Z)$ relations may be the most reasonable option provided that the type of the radar echo above the melting layer is determined using a polarimetric classification algorithm.

Figure 10a shows that the conventional relation (1) heavily underestimated rain at the surface if the hydrometeors in the radar resolution volume were identified as dry snow and crystals. Note that the classification routine allows for dry snow to be designated if part of the radar volume is below the freezing level. The errors are smaller at closer distances where the height of the radar resolution volume is at or below the freezing level (Fig. 10b). The Z measurements in these regions often closely resemble those in the rain beneath (e.g., Fabry and Zawadzki 1995). As the height of radar echo progressively increases with distance, rain underestimation becomes overwhelming (Fig. 10c).

To minimize the bias in the estimate of rain when dry snow/crystals are sampled by the radar at longer distances, we introduce an additional factor of 2.8 to conventional $R(Z)$ relation (1):

$$R(Z) = 2.8R(Z) = (4.76 \times 10^{-2})Z^{0.714}. \quad (4)$$

The intercept in (4) is between the intercepts of the Z - S relations recommended by Super and Holroyd (1998):

$$S = (3.86 \times 10^{-2})Z^{0.5}, \quad (5)$$

and by Vasiloff (2001):

$$S = (5.46 \times 10^{-2})Z^{0.5}, \quad (6)$$

for estimating snow water equivalent rate S on the operational NEXRAD network if snow near the surface is dry.

The performance of the conventional $R(Z)$ relation for a limited subset of cases in which the radar echo was classified as graupel/hail above the freezing level is il-

lustrated in Fig. 11. Because K_{DP} and Z_{DR} are usually small for dry graupel and hail aloft, it is hard to expect rainfall estimation improvement if these two polarimetric variables are used directly. Instead, we recommend using the modified $R(Z)$ relation for graupel/hail aloft with the multiplying factor 0.8, which minimizes the bias and rms error for this data subset.

4. Radar algorithms and their performance as a function of range

As shown in section 3, there is benefit in the use of different rainfall relations for different classes of radar echo. The idea of using multiple relations to optimize rainfall estimation as suggested by Chandrasekar et al. (1993), Cifelli et al. (2002), and Matrosov et al. (2005) was further explored by Ryzhkov et al. (2005b) in JPOLE studies. According to the “synthetic algorithm” developed by Ryzhkov et al. (2005b), the choice between various polarimetric rainfall relations is determined solely by the radar reflectivity Z or $R(Z)$ [i.e., rain rate computed from Z using (1)]. Ryzhkov et al. (2005b) recommend using the $R(Z, Z_{DR})$ relation in light rain [$R(Z) < 6 \text{ mm h}^{-1}$], the $R(K_{DP}, Z_{DR})$ relation in moderate-to-heavy rain [$6 < R(Z) < 50 \text{ mm h}^{-1}$], and the $R(K_{DP})$ relation in heavy rain [$R(Z) > 50 \text{ mm h}^{-1}$]. The three relations were optimized based on the comparison with the ARS gauges for rain events during JPOLE in 2002–03. In Ryzhkov et al. (2005b), the synthetic algorithm was validated only at distances of less than 90 km from the radar, where the contamination from mixed-phase and frozen hydrometeors is minimal. Note that the $R(Z, Z_{DR})$ relation in the synthetic algorithm is different from the one given by (3). The $R(Z, Z_{DR})$ relation in Ryzhkov et al. (2005b) was optimized for light rain where $R(Z) < 6 \text{ mm h}^{-1}$.

In this study, we use the approach of the synthetic algorithm using polarimetric classification rather than Z -based approaches, and it is applicable for a wide range of distances from the radar. This algorithm is constructed as follows:

$$\begin{aligned} R &= 0 \text{ if nonmeteorological echo is classified,} \\ R &= R(Z, Z_{DR}) \text{ if light/moderate rain is classified,} \\ R &= R(Z, Z_{DR}) \text{ if heavy rain or big drops are classified,} \\ R &= R(K_{DP}) \text{ if rain-hail is classified and range} < R_t, \\ R &= 0.6R(Z) \text{ if wet snow is classified,} \\ R &= 0.8R(Z) \text{ if graupel or rain-hail is classified and range} \geq R_t, \\ R &= R(Z) \text{ if dry snow is classified and range} < R_t, \text{ and} \\ R &= 2.8R(Z) \text{ if dry snow or crystals are classified and range} \geq R_t, \end{aligned} \quad (7)$$

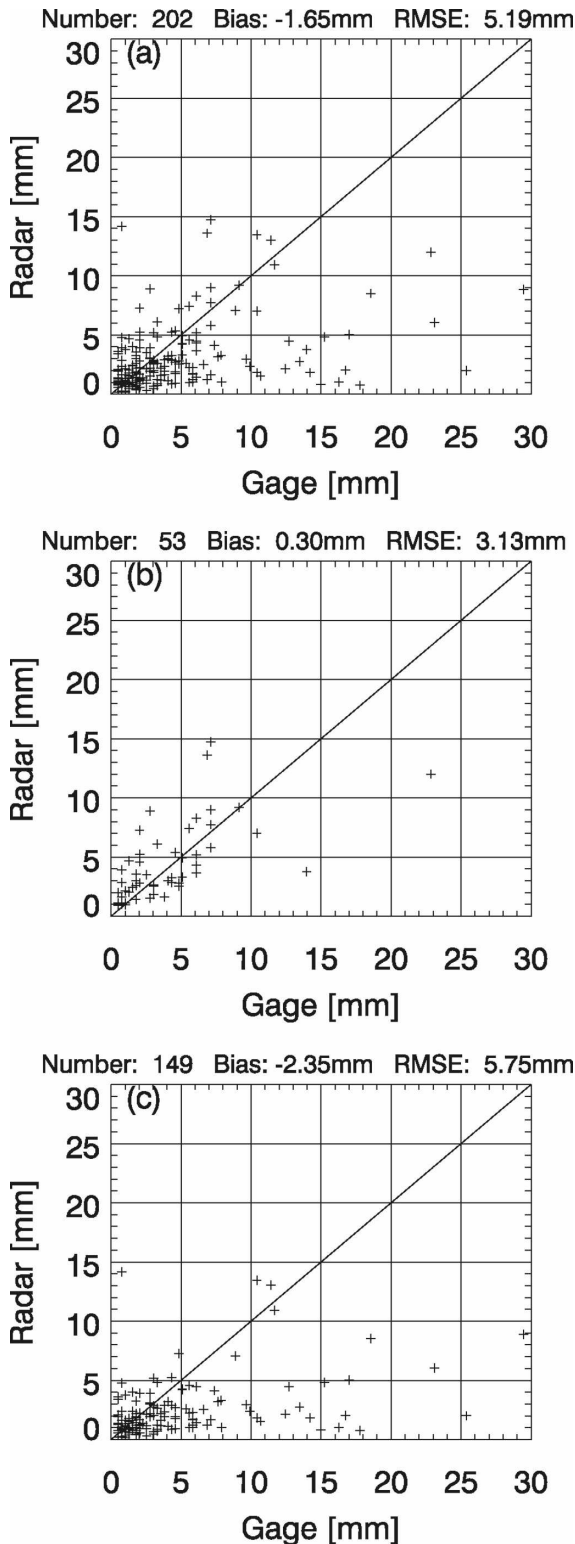


FIG. 10. Performance of the conventional algorithm for dry snow and crystals: (a) radar–gauge accumulation comparisons for all gauges, (b) comparisons for gauges at/below the geometric projection of the input melting level, and (c) comparisons at distances above the melting level.

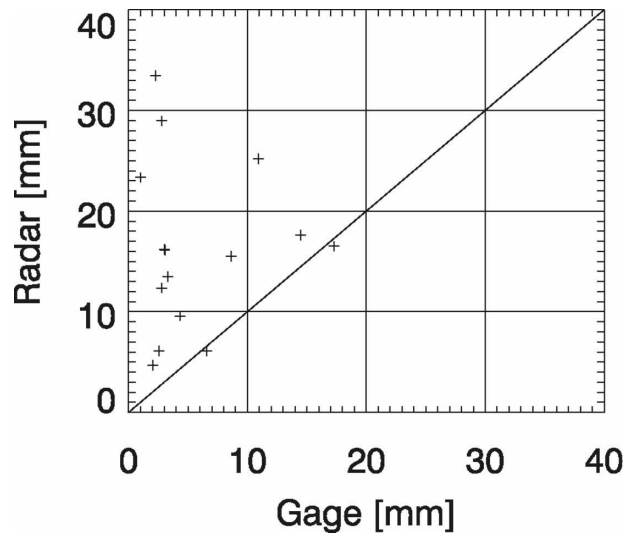


FIG. 11. Performance of the conventional $R(Z)$ algorithm if the radar volume is filled with graupel or hail and is located above the freezing level.

where the $R(Z)$, $R(Z, Z_{DR})$, and $R(K_{DP})$ relations are specified by (1)–(3) above, R_i is as specified in section 2, Z values are capped at 53 dBZ, and rain rate is set to zero if $\rho_{HV} < 0.85$ to ensure minimal contamination from nonmeteorological echoes. The set of equations in (7) composes an echo classification (EC) rainfall estimation algorithm. In the current version of the EC algorithm, we use two very different $R(Z)$ relations for dry snow below and above the freezing level. In the future, a more gradual change of the intercept parameter in the $R(Z)$ relation for dry snow/crystals as a function of range (or radar volume height) might be needed, similar to what was suggested by Hunter et al. (2001) for the WSR-88D snow accumulation algorithm or what is usually employed in the conventional VPR methods. This algorithm was tested on the entire dataset along with the individual relations (1)–(3) and the synthetic algorithm by Ryzhkov et al. (2005b).

The mean biases and RMS errors for five algorithms are plotted as functions of range for the entire dataset in Fig. 12. The distances from gauges have been partitioned into 50-km-wide range bins to smooth the plotting. Because of significant radar rainfall accumulations associated with intense convective lines (MCS) and hail-producing storms, convective warm-season events dominate the overall performance statistics in Fig. 12. Separate statistics were obtained for widespread “stratiform” rain events that we define as the events with an absence of convective signatures and for which the bright band played a significant role (Fig. 13). This subset includes 26 h of Oklahoma Mesonet gauge ob-

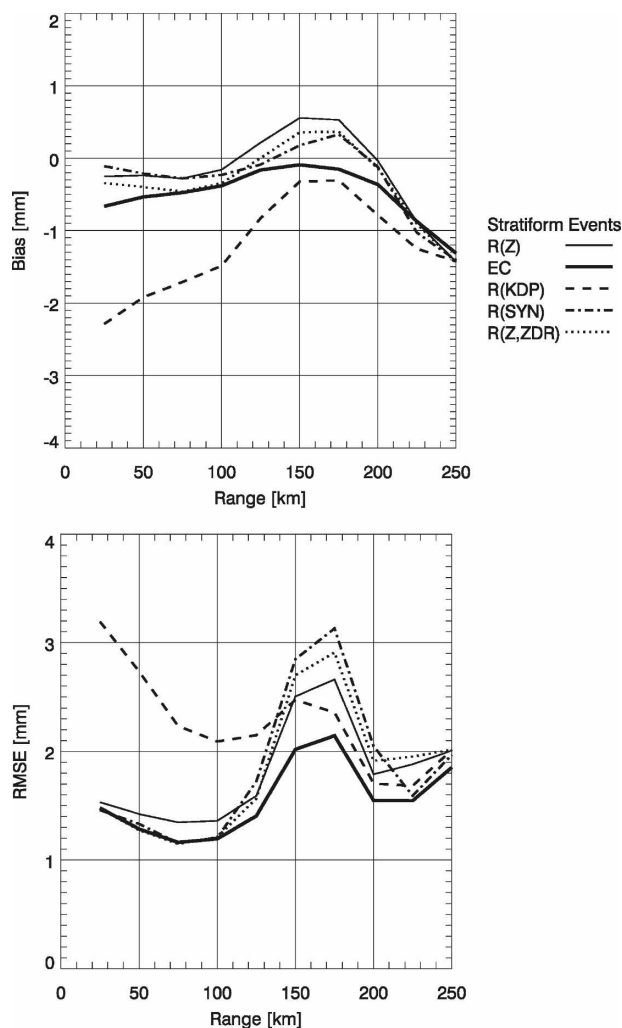


FIG. 12. (top) Mean bias and (bottom) RMS error of different radar estimates as a function of range (43 rain events, 179 h of observation).

servations during nine widespread cold-season precipitation events.

As was claimed by Ryzhkov et al. (2005c) and Giangrande and Ryzhkov (2003), the conventional WSR-88D algorithm tends to overestimate rainfall in a wide range of distances up to 200 km from the radar and underestimate it beyond 200 km because of the progressive overshooting of precipitation at longer ranges (Figs. 12, 13). The overestimation at ranges below 100 km is likely due to the impact of large drops and melting hail, which are very common in Oklahoma storms (Ryzhkov et al. 2005b). At ranges between 100 and 200 km, contamination from the bright band is another factor contributing to the positive bias of the conventional rainfall estimate. Depending on the height of the freezing level, the impact of the bright band is strongest in

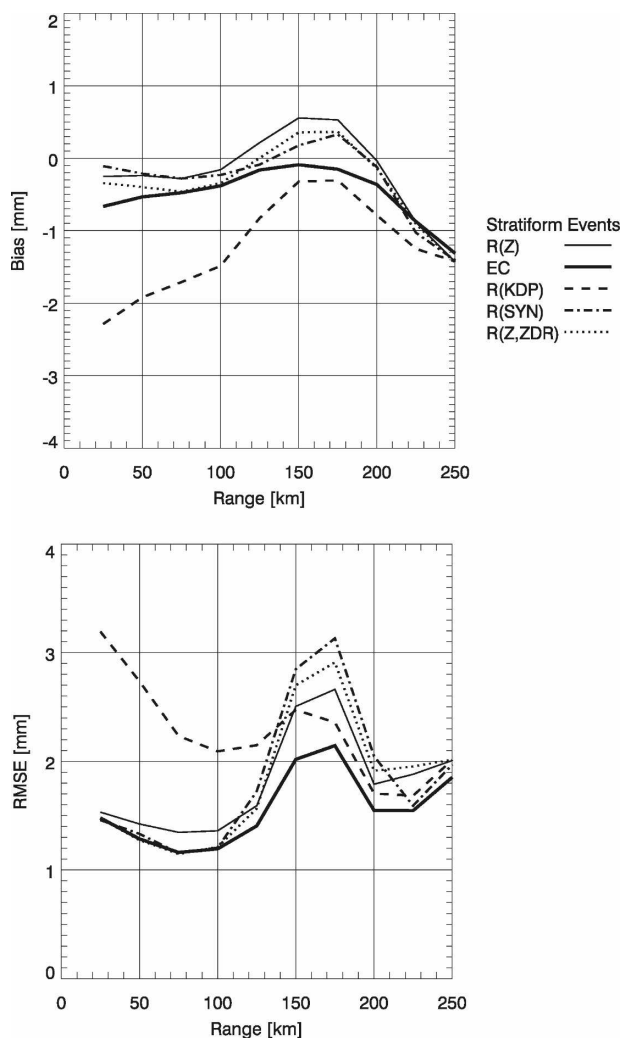


FIG. 13. As in Fig. 12, but for stratiform events with an absence of convective signatures (9 rain events, 26 h of observation).

the range interval of 130–180 km. Conclusions regarding the performance of the conventional WSR-88D $R(Z)$ relation in this paper are consistent with the results of independent statistical study by Krajewski and Ciach (2005), who examined a massive amount of radar data collected by the operational KTLX WSR-88D radar in the same region (i.e., central Oklahoma).

The performance of rainfall relations at close distances from the radar (<100 km) reaffirms initial JPOLE findings, which suggest that polarimetric methods and synthetic algorithms in particular outperform the conventional $R(Z)$ relation for most precipitation regimes. Three polarimetric algorithms, the Ryzhkov et al. (2005b) synthetic, EC-based, and $R(K_{DP})$, demonstrate similar performances at the ranges up to 130 km, with the EC algorithm producing the lowest bias and

the synthetic one yielding the smallest rms errors for all rain events combined (Fig. 12).

The EC algorithm significantly outperforms others in the range interval between 130 and 200 km in terms of the rms error. However, this result is not necessarily surprising because the tuned $R(Z)$ relations in mixed-phase and frozen hydrometeors in the proposed EC method (7) were developed by minimizing the bias and rms errors using subsets associated with different hydrometeor classes within the same multiyear dataset. Although our 4-yr dataset is large and encompasses a variety of different storms, independent testing and validation of the method in different climate regions is required to check stability of the suggested $R(Z)$ relations for nonrain hydrometeors. However, there is little chance to find a single $R(Z)$ relation that will perform satisfactorily for all classes of mixed-phase and frozen hydrometeors. Polarimetric classification combined with the use of multiple $R(Z)$ relations provides a better opportunity to reduce uncertainty in rainfall measurements in a wide range of distances from the radar.

Utilizing the classification-based polarimetric algorithm (EC) instead of the conventional $R(Z)$ relation results in a reduction of the bias and rms errors of hourly rainfall estimates up to 200 km from the radar (Figs. 12, 13). At distances within 50 km, the rms error is reduced by roughly a factor of 2, largely attributed to improved polarimetric performance in the presence of heavy rain and convective echo. This result echoes findings by Ryzhkov et al. (2005b), who reported a reduction by a factor of 1.7 for the cases observed in central Oklahoma during JPOLE. The improvement gradually phases out with increasing distance from the radar. The degree of the rms error reduction exceeds 50% at ranges up to 140–150 km and drops to about 20% at 200 km.

For the cold-season, nonconvective events, the EC algorithm also outperforms the conventional one, but to a lesser degree. Polarimetric methods capitalizing on the combined use of Z and Z_{DR} offer only modest improvement at close ranges. The most tangible improvement is achieved at longer distances from the radar where the impact of the bright band is maximal (Fig. 13).

While utilizing hydrometeor classification apparently improves the quality of rainfall estimation as compared with the stand-alone conventional relation $R(Z)$, one has to be aware of certain limitations of the suggested method. The errors in hydrometeor classification may introduce additional uncertainties and biases in rainfall estimation. Several important issues of class identification have to be addressed in future studies. Here we

illustrate the complexity of the problem with two examples.

What is the appropriate class designation from the standpoint of rainfall estimation if the radar resolution volume is filled with hydrometeors of two different types? A dual-polarization radar easily detects bright-band contamination when wet snow and rain coexist within the radar volume. Because wet snow exhibits a strong polarimetric signature, the classification algorithm may qualify the dominant scatterers in the volume as “wet snow” even if wet snow constitutes only a relatively small proportion of the scatterers. In such a situation, the use of the conventional $R(Z)$ relation for pure raindrops may be more appropriate than the wet-snow relation because Z is generally less sensitive to melting hydrometeors than are Z_{DR} or ρ_{HV} .

The impact of a wrong classification on rainfall estimation at longer distances from the radar is less dramatic if “fudge factors” in the modified $R(Z)$ relations for different classes of hydrometeors do not differ much. In the case of dry snow/crystals, this multiplicative factor changes abruptly from 1.0 to 2.8 at the distance R , according to (7). A more gradual transition will be implemented in a next version of the algorithm similar to what Hunter et al. (2001) suggested with respect to the WSR-88D snow accumulation algorithm.

The EC algorithm is designed to use specific differential phase K_{DP} more sparingly than is the synthetic algorithm, which implies more aggressive use of K_{DP} . This is dictated by the need to mitigate noisiness in rain fields and the appearance of negative accumulations related to noisy and negative K_{DP} . However, in some instances the K_{DP} -based algorithms may produce less bias if substantial averaging over time and space is performed. For example, the synthetic algorithm shows slightly smaller bias at shorter distances than the EC algorithm. Nevertheless, we believe that the overall performance of the EC algorithm is satisfactory and that the approach is well suited for implementation on the polarimetric NEXRAD. An advantage of the EC-based method is that it can be adapted to incorporate the ideas of traditional VPR correction, which will benefit from polarimetric classification.

5. Summary

The performance of the conventional and various polarimetric algorithms for rainfall estimation has been validated at a wide range of distances from the radar. This was accomplished using a large dataset that included radar data collected with polarimetric prototype of the WSR-88D radar and gauge data from the ARS Micronet and Oklahoma Mesonet networks in Oklaho-

ma. The type of radar echo in the radar resolution volume over gauge locations was identified using the polarimetric classification algorithm. The accuracy of rainfall estimation was assessed separately for different classes of radar echo, including liquid, mixed-phase, and frozen hydrometeors.

A new algorithm that utilizes multiple polarimetric relations and modified $R(Z)$ relations depending on a radar echo class has been developed. According to this strategy, quantitative precipitation estimation should be preceded by and contingent on results of hydrometeor classification. The $R(Z, Z_{DR})$ relation is utilized if the radar echo is classified as rain, and the $R(K_{DP})$ relation is used if large hail is mixed with rain. At longer distances, where the radar resolution volume is filled with mixed-phase and frozen hydrometeors, the polarimetric radar is primarily used as a classifier. The $R(Z)$ relations with additional multiplicative factors (or intercept parameters) are applied if the radar scatterers are identified as wet snow, dry snow, or crystals, as well as graupel and hail above the melting layer. These factors were optimized for our dataset, and further testing of the method using independent data in different climate regions will be needed to assess their variability. We do not exclude that in the future the $R(Z)$ relations should be modified according to the height of the radar resolution volume above ground or melting layer similar to the approach recommended by Hunter et al. (2001) for improvements of the WSR-88D snow accumulation algorithm.

A validation study that incorporates a 4-yr polarimetric dataset containing 43 rain events and 179 h of observations demonstrates that the performance of the suggested algorithm, which is based on echo classification (EC algorithm), is superior in terms of both bias and rms error. The most significant improvement, as compared with the conventional WSR-88D algorithm, is found in convective storms where the rms error of the hourly rain estimate is reduced by a factor of 2 at distances of less than 50 km from the radar.

The degree of improvement for all relations gradually decreases with range and becomes insignificant at distances beyond 200 km. It is shown that the EC method exhibits better performance than the conventional WSR-88D algorithm with a reduction by a factor of 1.5–2 in the rms error of 1-h rainfall estimates up to distances of 150 km from the radar. In regions with brightband contamination, the rms error for the EC method is reduced by a factor of 1.25 as compared with the conventional method. Only modest improvement in rms error is observed relative to the conventional relation in snow above the melting layer.

As opposed to the synthetic algorithm suggested by

Ryzhkov et al. (2005b), the EC algorithm uses specific differential phase K_{DP} sparingly. This was done to avoid noisiness inherent to most of the K_{DP} -based algorithms.

Acknowledgments. The authors thank Terry Schuur and Kevin Scharfenberg of NSSL for reading the manuscript and making useful comments on it. The authors also thank Rob Cifelli (CSU) and the two anonymous reviewers for a thorough review of the manuscript. Funding was provided by NOAA/Office of Oceanic and Atmospheric Research under NOAA-University of Oklahoma Cooperative Agreement NA17RJ1227, U.S. Department of Commerce. Part of this work was supported by the National Weather Service, the Federal Aviation Administration, and the NEXRAD Product Improvement Program. We express our gratitude to the staff of the Oklahoma Climatological Survey for providing high-quality gauge data. Continued funding for maintenance of the Oklahoma Mesonet is provided by the taxpayers of Oklahoma through the Oklahoma State Regents for Higher Education. The support from the NSSL and CIMMS, University of Oklahoma, staff who maintain and operate the KOUN WSR-88D polarimetric radar is also acknowledged.

REFERENCES

- Andrieu, H., and J. D. Creutin, 1995: Identification of vertical profiles of radar reflectivity for hydrological applications using an inverse method. Part I: Formulation. *J. Appl. Meteor.*, **34**, 225–239.
- Austin, P. M., 1987: Relation between measured radar reflectivity and surface rainfall. *Mon. Wea. Rev.*, **115**, 1053–1070.
- Aydin, K., Y. Zhao, and T. Seliga, 1990: A differential reflectivity radar hail measurement technique: Observations during the Denver hailstorm of 13 June 1984. *J. Atmos. Oceanic Technol.*, **7**, 104–113.
- Brandes, E. A., G. Zhang, and J. Vivekanandan, 2002: Experiments in rainfall estimation with a polarimetric radar in a subtropical environment. *J. Appl. Meteor.*, **41**, 674–685.
- Bringi, V. N., and V. Chandrasekar, 2001: *Polarimetric Doppler Weather Radar: Principles and Applications*. Cambridge University Press, 636 pp.
- Brock, F. V., K. C. Crawford, R. L. Elliott, G. W. Cuperus, S. J. Stadler, H. L. Johnson, and M. D. Eilts, 1995: The Oklahoma Mesonet: A technical overview. *J. Atmos. Oceanic Technol.*, **12**, 5–19.
- Chandrasekar, V., V. Bringi, N. Balakrishnan, and D. Zrnić, 1990: Error structure of multiparameter radar and surface measurements of rainfall. Part III: Specific differential phase. *J. Atmos. Oceanic Technol.*, **7**, 621–629.
- , E. Gorgucci, and G. Scarchilli, 1993: Optimization of multiparameter radar estimates of rainfall. *J. Appl. Meteor.*, **32**, 1288–1293.
- Ciach, G. J., 2003: Local random errors in tipping-bucket rain gauge measurements. *J. Atmos. Oceanic Technol.*, **20**, 752–759.

- Cifelli, R., W. A. Petersen, L. D. Carey, S. A. Rutledge, and M. A. F. Silva Dias, 2002: Radar observations of the kinematic, microphysical, and precipitation characteristics of two MCSs in TRMM LBA. *J. Geophys. Res.*, **107**, 8077, doi:10.1029/2000JD000264.
- Doviak, R. J., and D. S. Zrnić, 1993: *Doppler Radar and Weather Observations*. Academic Press, 562 pp.
- Duchon, C. E., and G. R. Essenberg, 2001: Comparative rainfall observations from pit and aboveground rain gauges with and without wind shields. *Water Resour. Res.*, **37**, 3253–3263.
- Fabry, F., and I. Zawadzki, 1995: Long-term observations of the melting layer of precipitation and their interpretation. *J. Atmos. Sci.*, **52**, 838–851.
- , G. L. Austin, and D. Tees, 1992: The accuracy of rainfall estimates by radar as a function of range. *Quart. J. Roy. Meteor. Soc.*, **118**, 435–453.
- Fiebrich, C. A., D. L. Grimsley, R. A. McPherson, K. A. Kesler, and G. R. Essenberg, 2006: The value of routine site visits in managing and maintaining quality data from the Oklahoma Mesonet. *J. Atmos. Oceanic Technol.*, **23**, 406–416.
- Giangrande, S. E., and A. V. Ryzhkov, 2003: The quality of rainfall estimation with the polarimetric WSR-88D radar as a function of range. Preprints, *31st Int. Conf. on Radar Meteorology*, Seattle, WA, Amer. Meteor. Soc., 357–360. [Available online at <http://ams.confex.com/ams/pdfpapers/64220.pdf>.]
- , and —, 2005: Calibration of dual-polarization radar in the presence of partial beam blockage. *J. Atmos. Oceanic Technol.*, **22**, 1156–1166.
- , J. M. Krause, and A. V. Ryzhkov, 2008: Automatic designation of the melting layer with a polarimetric prototype of the WSR-88D radar. *J. Appl. Meteor. Climatol.*, **47**, 1354–1364.
- Hunter, S. M., E. W. Holroyd, and C. L. Hartzell, 2001: Improvements to the WSR-88D snow accumulation algorithm. Preprints, *30th Int. Conf. on Radar Meteorology*, Munich, Germany, Amer. Meteor. Soc., 716–718. [Available online at <http://ams.confex.com/ams/pdfpapers/20852.pdf>.]
- Jameson, A. R., 1991: A comparison of microwave techniques for measuring rainfall. *J. Appl. Meteor.*, **30**, 32–54.
- Kitchen, M., 1997: Towards improved radar estimates of surface precipitation rate at long range. *Quart. J. Roy. Meteor. Soc.*, **123**, 145–163.
- Koistinen, J., 1991: Operational correction of radar rainfall errors due to the vertical reflectivity profile. Preprints, *25th Int. Conf. on Radar Meteorology*, Paris, France, Amer. Meteor. Soc., 91–94.
- Krajewski, W. F., and G. J. Ciach, 2005: Towards probabilistic quantitative precipitation WSR-88D algorithms: Data analysis and development of ensemble model generator: Phase 4. Office of Hydrologic Development Rep., NOAA Contract DG133W-02-CN-0089, 69 pp.
- Lim, S., V. Chandrasekar, and V. N. Bringi, 2005: Hydrometeor classification system using dual-polarization radar measurements: Model improvements and in situ verification. *IEEE Trans. Geosci. Remote Sens.*, **43**, 792–801.
- Liu, H., and V. Chandrasekar, 2000: Classification of hydrometeors based on polarimetric radar measurements: Developments of fuzzy logic and neuro-fuzzy systems, and in situ verification. *J. Atmos. Oceanic Technol.*, **17**, 140–164.
- Matrosov, S. Y., D. E. Kingsmill, B. E. Martner, and F. M. Ralph, 2005: The utility of X-band polarimetric radar for quantitative estimates of rainfall parameters. *J. Hydrometeorol.*, **6**, 248–262.
- May, P. T., T. D. Keenan, D. S. Zrnić, L. D. Carey, and S. A. Rutledge, 1999: Polarimetric radar measurements of tropical rain at a 5-cm wavelength. *J. Appl. Meteor.*, **38**, 750–765.
- McPherson, R. A., and Coauthors, 2007: Statewide monitoring of the mesoscale environment: A technical update on the Oklahoma Mesonet. *J. Atmos. Oceanic Technol.*, **24**, 301–321.
- Park, H.-S., A. Ryzhkov, D. Zrnic, and K. Kim, 2007: Optimization of the matrix of weights in the polarimetric algorithm for classification of radar echoes. Preprints, *33rd Conf. on Radar Meteorology*, Cairns, Australia, Amer. Meteor. Soc., P11B.4. [Available online at <http://ams.confex.com/ams/pdfpapers/123123.pdf>.]
- Ryzhkov, A. V., 2007: The impact of beam broadening on the quality of radar polarimetric data. *J. Atmos. Oceanic Technol.*, **24**, 729–744.
- , and D. S. Zrnić, 1995: Precipitation and attenuation measurements at a 10-cm wavelength. *J. Appl. Meteor.*, **34**, 2121–2134.
- , and —, 1996: Assessment of rainfall measurement that uses specific differential phase. *J. Appl. Meteor.*, **35**, 2080–2090.
- , S. E. Giangrande, V. M. Melnikov, and T. J. Schuur, 2005a: Calibration issues of dual-polarization radar measurements. *J. Atmos. Oceanic Technol.*, **22**, 1138–1155.
- , —, and T. J. Schuur, 2005b: Rainfall estimation with a polarimetric prototype of WSR-88D. *J. Appl. Meteor.*, **44**, 502–515.
- , T. J. Schuur, D. W. Burgess, P. L. Heinselman, S. E. Giangrande, and D. S. Zrnic, 2005c: The Joint Polarization Experiment: Polarimetric rainfall measurements and hydrometeor classification. *Bull. Amer. Meteor. Soc.*, **86**, 809–824.
- , and Coauthors, 2007: Comparison of polarimetric algorithms for hydrometeor classification at S and C bands. Preprints, *33rd Int. Conf. on Radar Meteorology*, Cairns, Australia, Amer. Meteor. Soc., P10B.3. [Available online at <http://ams.confex.com/ams/pdfpapers/123109.pdf>.]
- Sanchez-Diezma, R., I. Zawadzki, and D. Sempere-Torres, 2000: Identification of the bright band through the analysis of volumetric radar data. *J. Geophys. Res.*, **105**, 2225–2236.
- Seo, D.-J., J. Breidenbach, R. Fulton, D. Miller, and T. O'Bannon, 2000: Real-time adjustment of range-dependent biases in WSR-88D rainfall estimates due to nonuniform vertical profile of reflectivity. *J. Hydrometeorol.*, **1**, 222–240.
- Shafer, M. A., C. A. Fiebrich, D. S. Arndt, S. E. Fredrickson, and T. W. Hughes, 2000: Quality assurance procedures in the Oklahoma Mesonet. *J. Atmos. Oceanic Technol.*, **17**, 474–494.
- Smith, J. A., D.-J. Seo, M. L. Baeck, and M. D. Hudlow, 1996: An intercomparison of NEXRAD precipitation estimates. *Water Resour. Res.*, **32**, 2035–2045.
- Super, A. B., and E. W. Holroyd, 1998: Snow accumulation algorithm for the WSR-88D radar: Final report. Bureau of Reclamation Rep. R-98-05, Denver, CO, 75 pp.
- Vasiloff, S., 2001: WSR-88D performance in northern Utah during the winter of 1998–1999. Part I: Adjustments to precipitation estimates. NWS Western Region Tech. Attachment 01-02, 7 pp.
- Vivekanandan, J., D. S. Zrnić, S. M. Ellis, R. Oye, A. V. Ryzhkov, and J. Straka, 1999: Cloud microphysics retrieval using S-band dual-polarization radar measurements. *Bull. Amer. Meteor. Soc.*, **80**, 381–388.

- Wilson, J. W., and E. A. Brandes, 1979: Radar measurement of rainfall—A summary. *Bull. Amer. Meteor. Soc.*, **60**, 1048–1058.
- WSR-88D Radar Operations Center, 2001: WSR-88D system specification. Doc. 2810000D, 190 pp.
- Zawadzki, I. I., 1975: On radar-raingage comparison. *J. Appl. Meteor.*, **14**, 1430–1436.
- , 2006: Sense and nonsense in radar QPE. *Proc. Fourth European Conf. on Radar in Meteorology and Hydrology*, Barcelona, Spain, 121–124. [Available online at <http://www.grahi.upc.es/ERAD2006/>.]
- Zrnić, D. S., 1996: Weather radar polarimetry: Trends toward operational applications. *Bull. Amer. Meteor. Soc.*, **77**, 1529–1534.
- , and A. Ryzhkov, 1996: Advantages of rain measurements using specific differential phase. *J. Atmos. Oceanic Technol.*, **13**, 454–464.
- , and ———, 1999: Polarimetry for weather surveillance radars. *Bull. Amer. Meteor. Soc.*, **80**, 389–406.
- , ———, J. Straka, Y. Liu, and J. Vivekanandan, 2001: Testing a procedure for automatic classification of hydrometeor types. *J. Atmos. Oceanic Technol.*, **18**, 892–913.